Evolutionary Strategies for Identification and Validation of Material Model Parameters for Forming Simulations

Thomas Bäck
Natural Computing Group, LIACS - Universiteit Leiden
Niels Bohrweg 1
NL-2333 CA Leiden
+31 71 527 7108
baeck@liacs.nl

Lutz Keßler
ThyssenKrupp Steel Europe
Eberhardstraße 12
D-44145 Dortmund
+49 231 844 3009
lutz.kessler@thyssenkrupp.com

Ingo Heinle
BMW AG
Knorrstraße 147
D-80788 Munich
+49 89 382 31272
ingo.heinle@bmw.de

ABSTRACT
Identification and validation of material models for forming simulations to match experimental data is a key requirement of complex forming applications in the automotive industry. Besides the fact that these models need more and relatively expensive material data input, a problem is still the reliable fit of all necessary parameters. For the steel grade DX54, an interaction of strain rate and yield locus has been identified, finally leading to different material model calibrations. An even better accuracy of feasibility studies is promoted by using advanced yield locus models for forming simulations. With a new set of specially designed experiments in combination with evolutionary strategies, inverse material parameter identification is realized through minimization of a nonlinear error function. This approach defines a new and powerful method for selection and validation of the adequate material model for industrial simulation.

Categories and Subject Descriptors
J.2 [**Physical Science and Engineering**]: Engineering - SCR

General Terms
Experimentation, Standardization, Verification.

Keywords
Sheet Forming, Material Characterization, FEM, Optimization

1. INTRODUCTION
The demands for a high quality forming simulation have been emphasized by the introduction of various new materials with often restricted formability. To allow a high flexibility in modelling, a large number of theories have been implemented in different finite element codes. With respect to material aspects, feasibility studies with the help of forming simulations are characterized by the hardening rule, yield locus and the failure criteria applied. In daily practice, the strain distribution is mostly compared with the forming limit curve (FLC).

GECCO'11, July 12–16, 2011, Dublin, Ireland.

In addition, the friction law, the Young's modulus, in particular for spring-back requirements, and the modelling of a combined isotropic–kinematic hardening all play an important role. During the design phase of robust processes, the awareness of the simulation quality has to be assured. This can partly be done by calibrating the material model to different experiments. Figure 1 illustrates two different processes for calibration of finite element material models. The straight forward process is a linear combination of material selection, testing, modelling and application. This process is often applied when using the model of Hill ´48 and hardening functions by Swift or Voce [11]. It starts with simple measurements of a hardening curve, of R values (a measure of the plastic anisotropy of a rolled sheet material) by a tensile test and additionally the forming limit curve (FLC). The modelling is simple and the yield locus shape obeys the experimentally measured values. The hardening results directly from the chosen hardening formula. The risk of this strategy is an unqualified simulation due to material behaviour during forming, which is not in full correlation to the assumptions selected. Because of this, a validation phase with a simulation and real part result comparison is often introduced as a quality check.

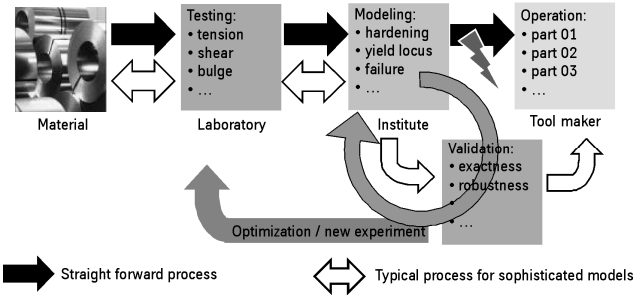

Figure 1: Material model calibration process

In order to allow the use of more sophisticated and flexible models, like Barlat 2000 or Banabic 2005 [4], the straight forward process needs some widening. To determine all the material model parameters needed, more experiments have to be added in the testing phase. After the test results have been interpreted, a model can be selected by comparing the predicted values of stress and anisotropy with the measurements in the modelling phase. Unfortunately, the result of this modelling process is not necessarily unique. The left-hand side of figure 2 shows the result for mild steel. Based on experiments from tensile tests and hydraulic bulge tests, the yield locus shape is plotted for three

different models. The biaxial stress point has been calculated using the method described in [5]. Hill ´48 does not agree with this point and predicts higher stresses in the biaxial stress state. Nevertheless, the models of Hill ´90 or Banabic 2005 compared here fully correspond to the experimentally determined value. With the value of m=6 [4] for steels, which is often given in the literature, the difference of both more flexible models concentrates in the area around $\sigma_{11} = 2\,\sigma_{22}$. The effect of this small difference of 3% is shown on the right hand side for a forming simulation with a door inner. By using the model of Hill ´48, a very safe process is assumed. No necking is expected. In contrast to this result, the yield locus of Hill ´90 predicts an unstable process and possible necking, whereas the fit of the Banabic 2005 model to the testing results, with the reported value of m = 6 for the shape, predicts a part with a larger rupture. To obtain a forecast similar to that given by Hill ´90 for the critical area, the drawing depth would have to be reduced by 1.5 mm for this model.

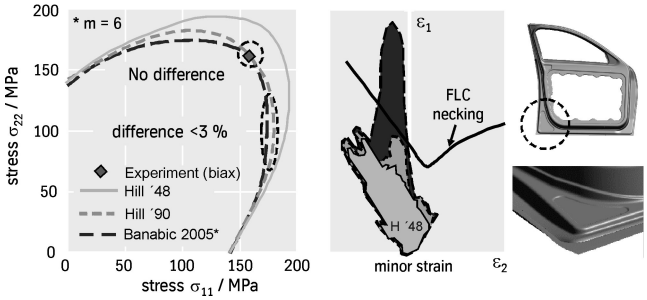

Figure 2 Impact of a yield locus selection on a door inner feasibility study

The example given here shows the challenge of designing a process for the material data calibration with respect to industrial forming simulation. Parameters of this process are time, money and validity of the simulation results for a wide selection of different parts. Even one or more extra experimental values, not focused to the uniaxial stress state, need to be analyzed carefully when selecting the final model based on this data. A new approach for parameter identification based on using evolutionary strategies and a systematic validation phase is discussed below.

2 MATERIAL MODELLING

Several yield loci models for anisotropic materials like Hill ´48 [11], Barlat ´89 [7], Barlat 2000 [8], Banabic 2005 [2] and Dell 2006 [8] have been proposed. Each yield locus model comprises parameters for modelling the desired material. The parameters are obtained by the minimization of the difference between a finite number of predicted and measured stress states and strain ratios (R values). In contrast to the Hill ´48 yield locus, those models published in the last decade offer more parameters, which enable better adaptation to the measured quantities. The drawback of the latter mentioned yield loci is the necessity of additional experiments for identifying all of the model parameters. Usually, the tensile, hydraulic bulge and shear tests serve the measured quantities. These experiments will be referred to as fundamental experiments. In this work, the flow curve $Y_{(\bar{\eta})}$ is obtained by a tensile test in the rolling direction and complemented by a bulge test for high strain states [5]. Furthermore, the hardening is assumed to be isotropic and the results of the fundamental experiments are assumed to be sufficiently stable and accurate. The accumulated plastic strain $\bar{\eta}$ [2] is given by

$$\bar{\eta} = \int \dot{\bar{\eta}}\,dt \quad \dot{\bar{\eta}} = \frac{\sigma : d^p}{\bar{\sigma}} \quad (1)$$

where σ is the Cauchy stress tensor and d^p is the rate of deformation. The effect of strain rate can be described by the strain rate sensitivity m [10]. Two tensile tests, performed under different rates (D, dynamic; S, static), are needed in order to identify the model parameter m.

$$m = \ln\left(\frac{Y_D}{Y_S}\right) / \ln\left(\frac{\dot{\bar{\eta}}_D}{\dot{\bar{\eta}}_S}\right) \quad (2)$$

The subsequent investigations are based on the plane stress yield loci Barlat ´89 and Barlat ´2000. For the following equations, the plane stress Cauchy stress tensor is defined in the axis system of the anisotropy. The Barlat ´89 yield locus may be written in the following form:

$$F(\sigma,\bar{\eta}) = \bar{\sigma}(\sigma) - Y_{(\bar{\eta})} = \left(\frac{1}{2}\left[a|K_1 + K_2|^m + a|K_1 - K_2|^m + c|2K_2|^m\right]\right)^{\frac{1}{m}} - Y_{(\bar{\eta})} \le 0 \quad (4)$$

$$K_1 = \frac{\sigma_{xx} + h\sigma_{yy}}{2} \quad K_2 = \sqrt{\left(\frac{\sigma_{xx} - h\sigma_{yy}}{2}\right)^2 + p^2\sigma_{xy}{}^2} \quad (5)$$

The Barlat ´89 yield locus reduces to the function proposed by Hill (1948) for the exponent of $m = 2$. The parameters a, c, h and p, which describe the anisotropy of the material, can be obtained from measured R values of tensile tests in three different directions.

In the case of the Barlat 2000 yield locus, the anisotropy of the material is modelled by a linear transformation of the stress tensor. The transformation itself is defined by the parameters α_i, which have to be determined for each material.

$$\begin{bmatrix} L'_{11} \\ L'_{12} \\ L'_{21} \\ L'_{22} \\ L'_{66} \end{bmatrix} = \frac{1}{3}\begin{bmatrix} 2 & 0 & 0 \\ -1 & 0 & 0 \\ 0 & -1 & 0 \\ 0 & 2 & 0 \\ 0 & 0 & 3 \end{bmatrix}\begin{bmatrix} \alpha_1 \\ \alpha_2 \\ \alpha_7 \end{bmatrix} \quad \begin{bmatrix} L''_{11} \\ L''_{12} \\ L''_{21} \\ L''_{22} \\ L''_{66} \end{bmatrix} = \frac{1}{9}\begin{bmatrix} -2 & 2 & 8 & -2 & 0 \\ 1 & -4 & -4 & 4 & 0 \\ 4 & -4 & -4 & 1 & 0 \\ -2 & 8 & 2 & -2 & 0 \\ 0 & 0 & 0 & 0 & 9 \end{bmatrix}\begin{bmatrix} \alpha_3 \\ \alpha_4 \\ \alpha_5 \\ \alpha_6 \\ \alpha_8 \end{bmatrix} \quad (6)$$

$$\begin{bmatrix} X'_{xx} \\ X'_{yy} \\ X'_{xy} \end{bmatrix} = \begin{bmatrix} L'_{11} & L'_{12} & 0 \\ L'_{21} & L'_{22} & 0 \\ 0 & 0 & L'_{66} \end{bmatrix}\begin{bmatrix} \sigma_{xx} \\ \sigma_{yy} \\ \sigma_{xy} \end{bmatrix} \quad \begin{bmatrix} X''_{xx} \\ X''_{yy} \\ X''_{xy} \end{bmatrix} = \begin{bmatrix} L''_{11} & L''_{12} & 0 \\ L''_{21} & L''_{22} & 0 \\ 0 & 0 & L''_{66} \end{bmatrix}\begin{bmatrix} \sigma_{xx} \\ \sigma_{yy} \\ \sigma_{xy} \end{bmatrix} \quad (7)$$

Finally, the yield locus is formulated in the principal space of the transformed stress tensor.

$$\phi' = |X'_1 - X'_2|^a \quad \phi'' = |2X''_2 + X''_1|^a + |2X''_1 + X''_2|^a \quad (8)$$

$$F(\sigma,\bar{\eta}) = \bar{\sigma}(\sigma) - Y_{(\bar{\eta})} = \left(\frac{1}{2}(\phi' + \phi'')\right)^{\frac{1}{a}} - Y_{(\bar{\eta})} \le 0 \quad (9)$$

Because of its eight parameters, this formulation offers more flexibility than the Barlat ´89 yield locus in order to reflect the results of the fundamental experiments. For the determination of the parameters α_i, the following non-linear system of equations has to be solved [2].

$$\begin{aligned} &\bar{\sigma}(\sigma_{00},\alpha,\alpha_i) - Y_{(\bar{\eta}_0)} = 0 \quad \bar{\sigma}(\sigma_{45},\alpha,\alpha_i) - Y_{(\bar{\eta}_0)} = 0 \quad \bar{\sigma}(\sigma_{90},\alpha,\alpha_i) - Y_{(\bar{\eta}_0)} = 0 \\ &\bar{\sigma}(\sigma_b,\alpha,\alpha_i) - Y_{(\bar{\eta}_0)} = 0 \\ &r_{00}(\sigma_{00},\alpha,\alpha_i) - r_{00}^{exp} = 0 \quad r_{45}(\sigma_{45},\alpha,\alpha_i) - r_{45}^{exp} = 0 \quad r_{90}(\sigma_{90},\alpha,\alpha_i) - r_{90}^{exp} = 0 \\ &r_b(\sigma_b,\alpha,\alpha_i) - r_b^{exp} = 0 \end{aligned} \quad (10)$$

A possible approach to solving this system is the formulation of an optimization problem. The corresponding objective function is shown in equation (11). The experimental results are equally weighted [BACP03].

$$\begin{aligned} f_{fit} = &\sum_{i=1}^{3}\left(\frac{\bar{\sigma}_{\alpha i} - Y_{(\bar{\eta}_0)}}{Y_{(\bar{\eta}_0)}}\right)^2 + \left(\frac{\bar{\sigma}_b - Y_{(\bar{\eta}_0)}}{Y_{(\bar{\eta}_0)}}\right)^2 \\ &+ \sum_{i=1}^{3}\left(\frac{r_{\alpha i} - r_{\alpha i}^{exp}}{r_{\alpha i}^{exp}}\right)^2 + \left(\frac{r_b - r_b^{exp}}{r_b^{exp}}\right)^2 \to \min \end{aligned} \quad (11)$$

3 EXPERIMENTS

In order to combine the material model identification and the validation phase, a set of experiments has been developed. The main objective of the test and tool design is to clarify hard-to-measure yield locus parameters. In prior studies, a significant impact of the yield locus shape, in combination with the selected hardening formulation, has been identified when the strain level comes near the FLC. The greatest impact of the yield locus shape occurred when complicated stretch forming conditions with different biaxial stress levels were oriented inside one geometrically defined stress path [5].

The essential elements of the proposed tests are online measurements of strain developments and the combination of different geometries with varying free areas of stretched material. BMW Group and ThyssenKrupp Steel Europe have jointly identified three different die face combinations to allow the simultaneous identification and validation of a yield locus shape exponent. The Yield Locus Identification Tool 1 of TKSE (YLIT 1 – TKSE) has a hemispherical punch in combination with a circular die opening. The punch diameter can vary between 20 mm and 80 mm and the die diameter should then measure 1.5 to 2.5 times the punch diameter. During testing, the rectangular or shaped sheet is fully clamped by a blank holder. The tooling is equipped with an on-line camera system for the strain measurement and a load cell for the force detection. At the end of a test, performed until a first visible necking is apparent, all areas of the blank can be analyzed with a strain measurement system to identify major strain directions and also strain combinations. It is also possible to derive an exact strain path history wherever the critical position develops. The YLIT 2 – TKSE and YLIT 3 – BMW Group are similar in geometry, but different in dimensions. By combining a square punch and a circular die opening, different stress states can be adjusted. A key function is the blank width selected for the experiment. The dimension of the punch ranges from 20 mm up to 100 mm and the die opening corresponds to 1.3 to 2.5 times the punch edge length. Again, the blank is fully clamped during the experiment and all process parameters can be recorded in a manner similar to the YLIT 1 – TKSE setup.

Figure 3 shows the fundamental specimen shape for YLIT 1 and YLIT 2. Both specimens are in the state of a visible localized necking. The location of necking is not in an area with tool contact for both experiments. This allows a free material flow in the highly stressed region. For the results discussed below, the strain development on the pole and at the necking zone is used. Additional strain combinations are given for discrete punch travel positions before the maximum strain reaches the FLC.

4 INVESTIGATIONS OF THE YLIT 1 – TKSE, YLIT 3 – BMW

The steel grade DX54 is taken as an example for the subsequent investigations. Hence, the presented results are only valid for the mentioned material. All discussed findings are based on the fundamental experiments, the chosen strategy for the computation of the equivalent plastic strains and the determination of the static flow curve. If a different hardening extrapolation would be selected, we assume that the conclusions would be different.

The punch position of the experiment, which is related to the beginning of the localized necking, is defined as the reference drawing depth. The failure evaluation on the basis of the forming limit curve (FLC) is a widely applied method for predicting the onset of necking instability, which is defined in the principal strain space and was originally introduced by Keeler [10] and Goodwin [14]. A material point is considered safe in terms of necking instability under the condition that the principal values of the associated strain tensor are below the curve. Provided the forming limit curve describes the material failure sufficiently accurately, an ideal material model should give, for the reference drawing depth, a principal strain tensor field, which does not exceed the FLC curve and contains regions which are close to the failure limit.

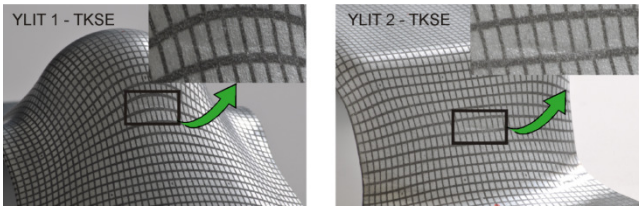

Figure 3: YLIT 1 and 2 specimen with the onset of a localized neck

Table 1 and table 2 show the reference drawing depth of the experiment and a selection of simulation results. According to the results depicted in figure 4, table 1 and 2, the exponent of the yield locus has a strong influence on the prediction of the drawing depth. Hence, the drawing depth can act as an indicator for the yield locus exponent. Some yield locus exponents predict a significantly different drawing depth for specimens, extracted in and perpendicular to the rolling direction (RD rolling direction; TD transverse direction). As a consequence, both types of specimens will be investigated in the subsequent sections. Furthermore, there is a noteworthy difference between those results obtained taking the strain rate dependency of the material hardening into account and those which are obtained without taking it into account. As opposed to the Barlat 2000 yield locus, the Barlat ´89 yield locus is able to predict the measured drawing depth with and without modelling strain rate dependency of the hardening effect ($m = 4.7$; $m = 3.2$). This result will be discussed again further below. Regarding the Barlat 2000 yield locus, a good prediction is obtained by an exponent of $a = 5.0$. The Barlat 2000 yield locus does not have an advantage if exponents below $a = 3$ are applied. Therefore, the exponent $a = 3$ is considered as a lower boundary for this material. Additionally, figure 5 illustrates the dependency of the position of the necking zone with respect to the yield locus exponent for the YLIT 3 – BMW. For the further investigations, additional measured quantities for the evaluation of the considered material models are introduced. First of all, the strain state in the centre of the necking zone is taken into account. The strain state is extracted on the basis of the punch position of 4 mm below the reference drawing depth. Finally, the punch force is also applied for comparing the simulation results with the measured data. The given forces are related to the same punch position as the strain states. Table 1 and table 2 show that two different exponents of the Barlat ´89 yield locus are able to predict the drawing depth in accordance with the experiment. As the strain increment during the simulation is derived from the yield locus, different yield locus shapes should lead to different strain states, which is confirmed by the results of table 3. The comparison of the

deviation between the computed and measured strain states shows (table 3) that the solution obtained by the strain rate dependent hardening model should be preferred. Provided the strain rate dependent hardening is applied, the prediction quality on the basis of both yield loci with respect to the introduced measured quantities is similar.

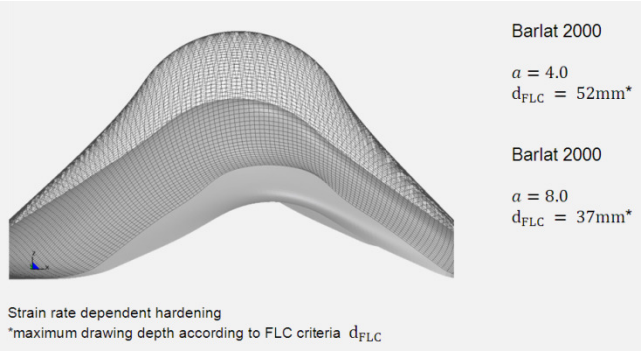

Figure 4: Comparison of the maximum drawing depths, YLIT 1 – TKSE

Table 1: Drawing depth, strain rate dependent hardening, YLIT 1 – TKSE

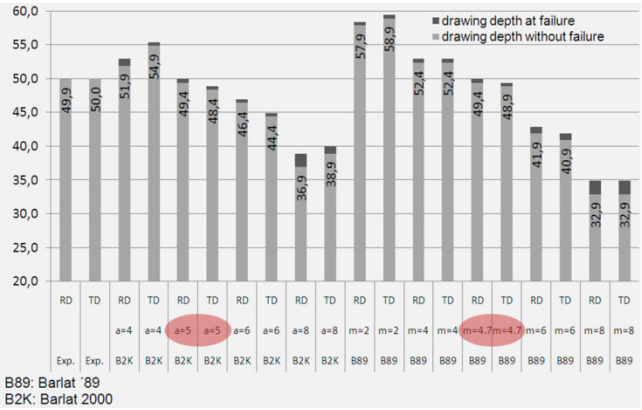

Table 2: Drawing depth, without strain rate dependent hardening,

YLIT 1 – TKSE

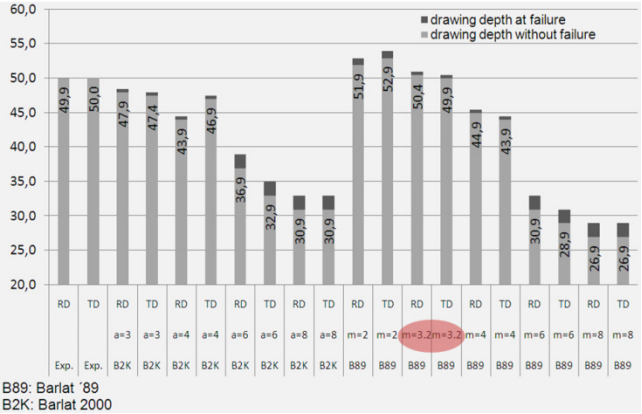

As the Barlat 2000 yield locus reflects the measured quantities of the fundamental results more accurately than the Barlat ´89 yield locus, the prediction of arbitrary stress states should be better. Therefore, if a choice has to be made, the Barlat 2000 yield locus could be preferred here. However, it has to be mentioned, that other yield loci containing a sufficient number of parameters, like Banabic 2005 or Dell 2006, should also be able to give similar results to the Barlat 2000 yield locus.

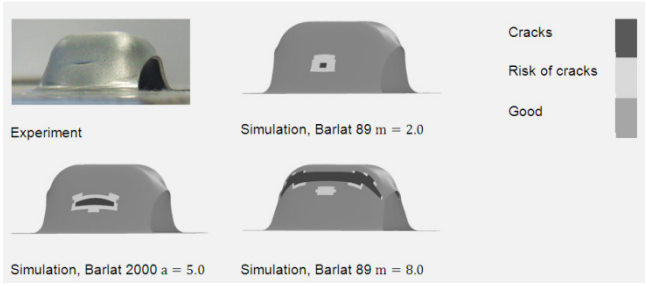

Figure 5: Different locations and shapes of localized necking, YLIT 3 – BMW

	φ_1		φ_2		$F_{punch}[kN]$	
	RD	TD	RD	TD	RD	TD
Experiment	0.52	0.55	-0.23	-0.26	35.1	35.7
Barlat 89; m=3.2 Strain Rate Dependency: off	0.62	0.59	-0.33	-0.33	34.5	36.2
Barlat 89; m=4.7 Strain Rate Dependency: on	0.53	0.51	-0.25	-0.25	34.5	37.2
Barlat 2000; a=5 Strain Rate Dependency: on	0.57	0.53	-0.27	-0.25	34.2	35.6
Barlat 89; m=2 Strain Rate Dependency: on	0.57	0.56	-0.33	-0.33	35.1	36.9

Table 3: Results of the subsequent necking zone, YLIT 1 – TKSE

5 OPTIMIZATION

According to the presented results, a potential of determining the yield locus exponent by an inverse approach, is recognisable. The exponent is derived indirectly from the lowest possible deviation between the simulation results and the measured data. The described task can be formulated as an optimization (minimization) problem. Thereby, the objective function measures the difference between the simulation and the measured data. Additionally, it also is necessary to answer the question as to whether friction has a strong influence on the simulation results. For answering this question, the sensitivity of the friction coefficient will be analyzed on the basis of the optimization results. The time consumption for the optimization is determined by the computation time of an objective function evaluation, which lies in this case, between an hour and two hours, and the soft- and hardware resources. Therefore, an optimization strategy is preferred, which gives the desired result with a minimum of objective function evaluations. Additionally, an optimization strategy is needed, which allows a sensitivity analysis and is able to overcome local minima. Grid and gradient methods are, therefore, not recommended. It is proposed to use evolutionary strategies for performing the optimization. Evolutionary strategies meet the mentioned demands and show a high robustness regarding nonlinearities. Hence, this approach seems to be a good

compromise in comparison to a full sampling, which is too expensive, and does not focus on the interesting parameter space regions. A comprehensive description of evolutionary strategies can be found in [Bäc96].

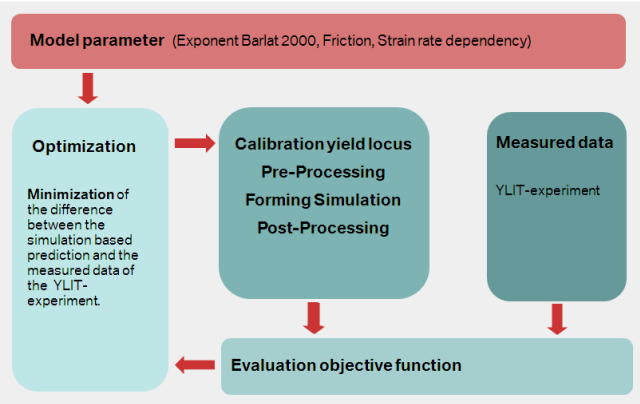

Figure 6: Identification model parameters

Figure 6 illustrates the scheme of the optimization for the determination of the yield locus exponent. As depicted, each optimization step comprises a calibration of the yield locus parameter α_i depending on the selected yield locus exponent a. As mentioned above, the identification of the yield locus parameter can be performed on the basis of an optimization. As all the parameters α_i are real valued, the CMA-ES (Covariance Matrix Adaptation-Evolutionary Strategy) algorithm of Hansen [9] is applied. After the yield locus parameters are determined, the input files for the simulation are generated, the forming simulation is performed and the results are evaluated. Subsequently, the simulation results are prepared for the comparison with the measured data. Finally the value of the objective function is computed. The prediction quality of the material model is measured, as shown above, on the basis of the drawing depth and the prediction of the strain state in the necking zone. For treating this multiple objective problem a desirability function is applied, as there is not any conflict expected between the objectives. In this case, a prior knowledge regarding the link between the objectives is necessary. Expression (13) shows the applied two-sided Harrington desirability function [13].

$$d_i(Y') = e^{-|Y'|^n} \quad Y' = \frac{2Y - (U + L)}{U - L} \quad (13)$$

The objective function value is computed as shown by (14).

$$f = 1 - \prod_{i=1}^{k} d_i \quad (14)$$

Table 4 summarizes the parameters of the Harrington desirability function, which have been applied for linking the objectives. The values for the parameters have been chosen based on experience.

Table 4: Parameters Harrington desirability function

Parameter	Drawing depth	Strain state
U	4	0.2
L	-4	-0.2
n	2	4

For the drawing depth and for both principal values of the considered strain states a desirability function is defined. On the basis of these set of desirability functions for each specimen (in and perpendicular to the rolling direction) the objective function is calculated as shown by (14). Table 5 shows the domain of the yield locus exponent for the optimization and the additionally investigated parameters.

Table 5: Optimization parameters

	Parameter	Domain	Type
Material model	Strain rate dependency (SRD) (0 = off; 1 = on)	0 - 1	Discrete
Exponent Barlat 2000	a	3 - 8	Continuous
Process parameter	Friction	0.08 - 0.12	Continuous

For this optimization, an extended (1,λ)-evolutionary strategy [1] has been applied. Figure 7 depicts the result of the yield locus exponent identification. The best prediction of the strain state and the drawing depth is obtained by an exponent between 4.8 and 5.0. This range is derived from figure 7 by considering both, the best and the worst fitness value related to each yield locus exponent. The mentioned interval also implies fitness values of 1.0, which are ignored. The reason why these points are permissible is given below.

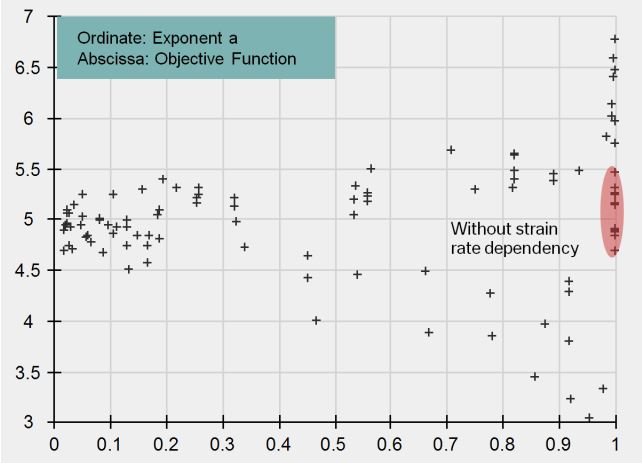

Figure 7: Identification model parameters, yield locus exponent

The determined exponent is in accordance with the investigations of chapter 4. The subsequent investigations are based on the exponent of 5.0. According to figure 8, friction does not play a crucial role for the prediction of the measured quantities of the investigated YLIT-experiment, because the optimum is obtained for friction coefficients between 0.08 and 0.11. As shown by table 2, the prediction of the drawing depth fails, if the strain rate dependency of the material is not considered. According to figure 9, satisfying results are only obtained under the consideration of the strain rate effect, which confirms the findings of table 2. All the objective function evaluations, which are performed without taking the strain rate depended hardening into account, lead to a fitness value of 1.0 independent of any other model parameter. Hence, figure 7 comprises even for a yield locus exponent between 4.8 and 5.0 fitness values of 1.0.

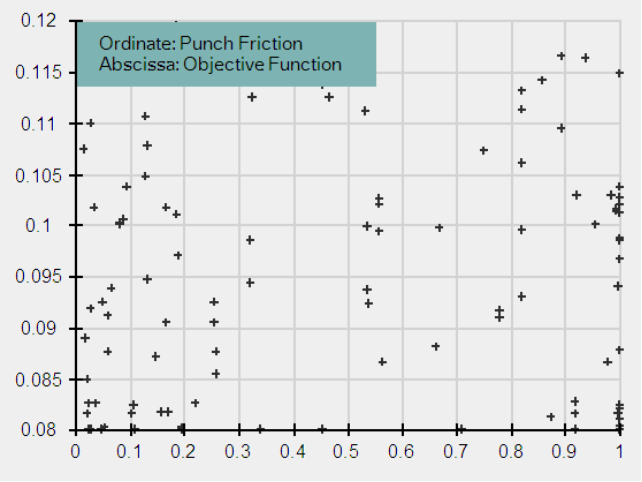

Figure 8: Identification model parameters, friction

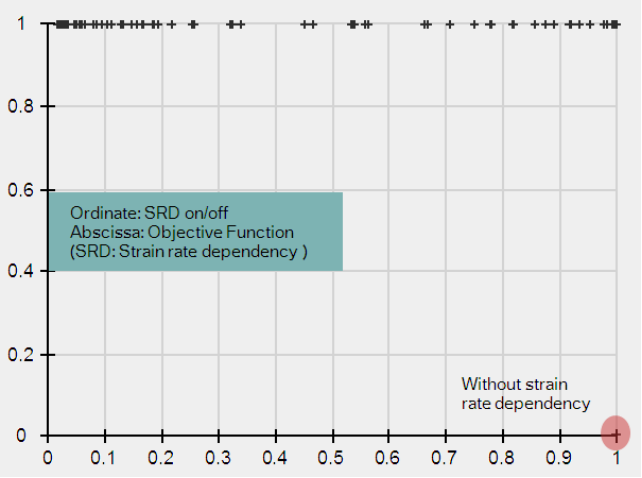

Figure 9: Identification model parameters, strain rate dependency

As mentioned above, for the calibration of the yield locus, the measured stress and strain state of the fundamental experiments are needed. Generally, the intrinsic values of these measured quantities are unknown. Additionally, further measured quantities are needed for the calibration of the hardening model and the elastic material model (table 6) like the Poisson's ratio or the strain rate sensitivity (m-Value), which are also obtained from the fundamental experiments. The so far presented results are based on a material model, implying the directly measured values from the fundamental experiments, which will be called standard material model calibration. Now, the question arises, whether the result of the inverse identification of the yield locus exponent is strongly affected by the uncertainty of the measured quantities derived from the fundamental experiments. A possible solution for investigating this question could be a design of experiments DOE of the measured quantities in the estimated range of their uncertainty. It has to be mentioned, that the determination of a confidence interval of the measured quantities is too expensive. Hence, the interval of the uncertainty is estimated on the basis of experience and the center of the interval is assumed to be coincident with the measured values. In this case, for each variation of the measured quantities, the best possible exponent would be determined.

Table 6: Allowed tolerances in the measured input data

Parameter	Range	Parameter	Range
σ_{00}	±1%	m-Value	±2%
σ_{45}	±1%	Scaling flow curve	±1%
σ_{90}	±1%	Shift flow curve	±1%
σ_B	±1%	Poisson's ratio	±5%
τ	±1%	Blank thickness	±1%
r_{00}	±5%	Velocity punch	±10%
r_{45}	±5%		
r_{90}	±5%		
The centre of the interval is coincident with the measured values and the given percentages refer to the same values.			
Shift flow curve	*The curve is shifted in direction of the stress axis.*		
Scaling flow curve	*The scaling of the flow curve is defined by a delta value, which refers to 1.5 equivalent plastic strain and scales the flow curve in the direction of the stress axis. The delta value is derived from the original flow curve at 1.5 equivalent plastic strain and the given percentage. The scaling eases at the yield strength.*		

Such an investigation would give the sensitivity of the measured quantities with respect to the inversely identified yield locus exponent. As a result, it would lead to a parameter space with fourteen dimensions. Under consideration of the commonly available hardware resources in an industrial environment, such a DOE based investigation would be too expensive.

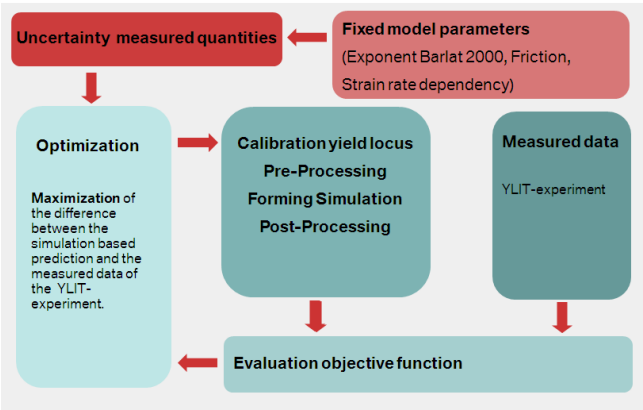

Figure 10: Investigation: uncertainty measured quantities

Hence, another approach is suggested. Instead of a DOE, an optimization problem can be formulated. The design space of the optimization is identical with the space defined by the measured quantities. The objective is to find a 14-dimensional vector of the measured quantities, which maximizes the deviation between the simulation result and the measured data of the YLIT experiment. Apart from transforming the minimization into a maximization, the same scheme is used as for the identification of the model parameter (Figure 10). For this optimization, the identified yield locus exponent (a=5.0) is used and the strain rate dependency of the material is considered. The remaining yield locus parameter are calibrated for each simulation within the optimization. As a result, the worst case regarding the influence of the uncertainty of

the measured quantities for the material model calibration on the simulation based prediction of the YLIT experiment is obtained. This approach is a compromise in order to perform the desired investigation by investing a minimum number of objective function evaluations. According to figure 11 a maximum has been found after 50 objective function evaluations. Figure 12 and 13 shows the development of the optimization parameters. The parameters are separated into two pictures in order to increase the clarity. The ranges of all the parameters are mapped into an interval between zero and one.

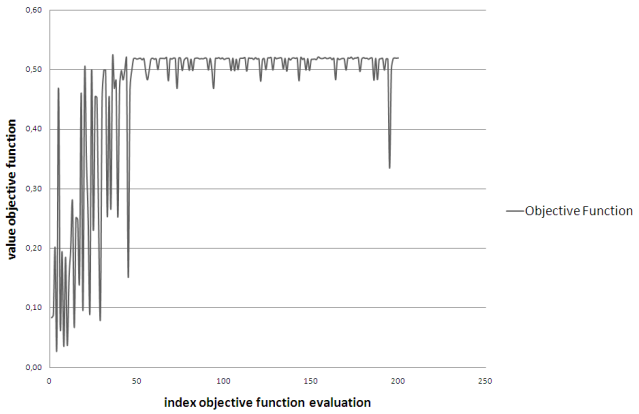

Figure 11: Investigation: uncertainty measured quantities, values objective function

Table 7: Investigation: uncertainty measured quantities, maximum deviation

	φ_1		φ_2		*Drawing Depth* [mm]	
	RD	TD	RD	TD	RD	TD
Experiment	0.52	0.55	-0.23	-0.26	50.0	50.0
Barlat 2000; a=5 Strain Rate Dependency: on *Standard material model calibration*	0.57	0.53	-0.27	-0.25	49.4	48.4
Barlat 2000; a=5 Strain Rate Dependency: on *Maximum deviation between simulation and measured data*	0.54	0.52	-0.27	-0.23	51.4	47.9

The worst case, identified by the optimization, is compared with the prediction of the simulation implying the standard material model calibration (table 7). Even under the worst possible set of measured quantities, obtained from the fundamental experiments, the results of the YLIT-experiment are predicted well. Consequently, the identified yield locus exponent gives satisfying results in the domain of the uncertainty of the fundamental experiments. One has to bear in mind that the uncertainty of the measured quantities has been assumed. Hence, a wider range of interval of the uncertainty could lead to worse results. Additionally, the center of the interval has been assumed to be coincident with the measured values.

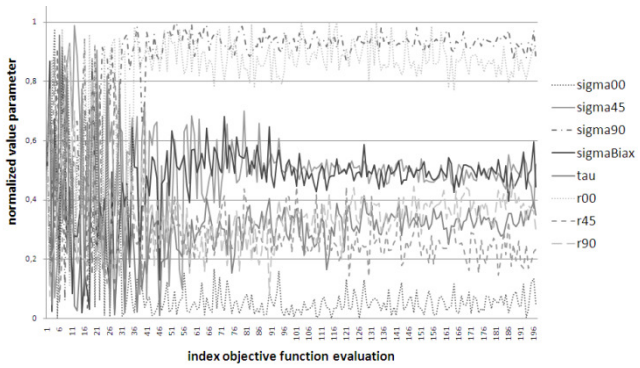

Figure 12: Investigation: uncertainty measured quantities, parameter propagation

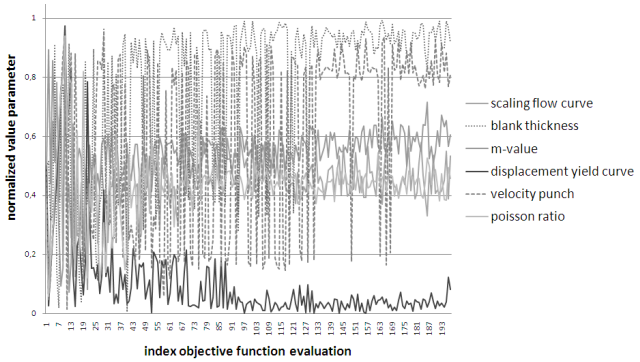

Figure 13: Investigation: uncertainty measured quantities; parameter propagation

6 VALIDATION BASED ON THE YLIT 2 - TKSE, YLIT 3 - BMW

The determination of the material model has been based on the experiment YLIT 1 – TKSE. As a material model should be able to predict the material behavior for arbitrary stress states, it is proposed to perform additional validation experiments.

In this work, the experiments YLIT 2 - TKSE, YLIT 3 – BMW act as validation experiments. According to table 8, the Barlat 2000 yield locus in combination with the exponent 5.0 gives a good prediction of the strain state in the necking zone. Again, as for the YLIT 1 – TKSE experiment, the strain states are taken before localized necking occurs. For the future, additional validation experiments should be considered in order to capture a wide range of stress states.

Table 8: Results of the subsequent necking zone

	YLIT 2 – TKSE		YLIT 3 – BMW	
	φ_1 ,RD	φ_2 ,RD	φ_1 ,TD	φ_2 ,TD
Experiment	0.41	-0.14	0.36	-0.14
Barlat 2000; a=5.0 Strain Rate Dependency: on	0.40	-0.17	0.36	-0.15
Barlat 89; m=2 Strain Rate Dependency: on	0.47	-0.25	0.36	-0.19

7 DISCUSSION AND OUTLOOK

The requirements for the quality of forming simulations are increasing. Each company has to balance the efforts of a material model calibration in combination with the validation work with respect to the requirements of the individual die making process. A final recommendation for one specific and individual material model or material model calibration can therefore not be given here. The following text discusses identified findings.

To date, it seems that the existing material modelling is sufficient for a large number of steel families. The generally applied model of Hill ´48 did not fulfil all YLIT-requirements in the best way and is therefore not the best choice when trying to operate near the FLC. To gain more accuracy by material modelling, one of the biggest challenges is the identification of the material parameters for the constitutive laws. This is especially true for the advanced material models with a larger number of parameters. Nevertheless, a variety of expensive non-standardized experiments allow a mathematical calibration procedure today. In this procedure, some areas of a yield locus still have to be defined by guessing or performing even more experiments (plane strain area). Unfortunately, the identified material model fit cannot directly be ranked with respect to the final result quality when simulating real industrial parts. Especially with advanced yield locus models, we identified a difference of the first parameter identification, fully on the basis of fundamental tests and the later final fit, by using optimization procedures and specially designed validation experiments. It therefore seems beneficial to include a well designed validation loop in this material modelling process, compare figure 1.

For hot-dip galvanized and electrolytically coated mild steel grades, in combination with an explicitly formulated FEM code, we summarize our findings as follows when applying them to the reference tools:

- With strain rate sensitivity, all experimental data (punch travel, strain distribution, necking location) are reproduced in a better, more realistic way. The simulation instability corresponds well with the experimental point of instability.
- Evolutionary strategies in combination with the selected validation experiments allow a fit of the yield locus shape function parameter and to date have given results.
- An optimization based approach is proposed in order to investigate the influence of the uncertainty of the measured quantities on the prediction of the simulation with respect to the YLIT-experiments.

The outcome of this investigation is a clear need to add well designed validation experiments or to safely identify parameters which are not directly derived from the fundamental tests. In this paper, we propose three different YLIT-experiments, with a relatively simple geometrical shape but complex material stressing. A clear reaction caused by the yield locus parameters has been identified by the specially designed experiments. Evolutionary strategies in combination with an appropriate objective function are a valuable approach for the cost-efficient identification of the yield locus parameter on the basis of the fundamental and the proposed experiments. This is because, as shown above, different measured quantities (drawing depth, strain state) have to be taken into account for assessing a yield locus and its parameters for a material. The formulation of an optimization problem makes it possible to determine the yield locus parameters automatically. As a next step, the complete material modelling process result has to be proven in the tool shop.

ACKNOWLEDGMENTS

The authors would like to thank all people, who supported the current work. Especially, we would like to gratefully thank Mr. Joerg Gerlach, Mr. Claus Strauß (both ThyssenKrupp Steel Europe) and Mr. Boris Bevc (BMW) for discussion and experimental support.

REFERENCES

[1] T. Bäck, *Evolutionary Algorithms in Theory and Practice*, Oxford University Press, New York, 1996

[2] D. Banabic, H. Aretz, D.S. Comsa and L. Paraianu, *An improved analytical description of orthotropy in metallic sheets*, vol Muncii no. 103-105, 2003

[3] D. Banabic et al.: An improved analytical description of orthotropy in metallic sheets, *Int. J. Plasticity*, 21(3): 493-512, 2005.

[4] D. Banabic, D.S. Comsa, M. Sester, M. Selig, et. al. Influence of constitutive equations on the accuracy of prediction in sheet metal forming simulation, *Numisheet 2008*, pp. 37-42, Interlaken, 2008

[5] T. Beier, J. Gerlach, L. Kessler and M. Linnepe, The Impact of Advanced Material Simulation Parameters in Press Shop Operations Using Mild Steel Grades, *SAE paper 2010-01-0992*, SAE World Congress 2010, Detroit

[6] F. Barlat, J. W. Yoon and O. Cazacu, On linear transformations of stress tensors for the description of plastic anisotropy, *International Journal of Plasticity 23*, S. 876–896, 2007

[7] F. Barlat and J. Lian, Plastic behavior and stretchability of sheet metals, Part I: A yield function for orthotropic sheets under plane stress conditions, *International Journal of Plasticity*, Vol. 5, pp. 51-66, 1989

[8] H. Dell, H. Gese and G. Oberhofer, *Users' Manual, MF GenYld + CrachFEM 3.8 Theory*, Munich, 2008

[9] N. Hansen, *The CMA Evolution Strategy: A tutorial*, 2008

[10] S.P. Keeler, Determination of forming limits in automotive stampings, *Society of automotive engineering sheet*, Paper Number: 650535, 1965

[11] R. Hill, A Theory of the Yielding and Plastic Flow of Anisotropic Metals, In: *Proceedings of the Royal Society of London. Series A*, Mathematical and Physical Sciences 193, 1948, S. 281-297, London, 1948

[12] J. C. Simo and T. J. R. Hughes, *Computational Inelasticity*, Springer, New York, 2000

[13] J. Harrington, The desirability function, *Industrial Quality Control 21 (10)*, pp. 494 – 498, 1965

[14] G.M. Goodwin, Application of Strain Analysis to Sheet Metal Forming Problems in the Press Shop, *Society of automotive engineers*, Paper Number: 68009, 196